IOP Conf. Series: Journal of Physics: Conf. Series **1219** (2019) 012021 doi:10.1088/1742-6596/1219/1/012021

Measurement of the neutrino oscillation parameters by NOvA

M A Acero[1]

[1] Programa de Física, Universidad del Atlántico, Puerto Colombia, Colombia

E-mail: marioacero@mail.uniatlantico.edu.co

Abstract. Using a beam made (mainly) by muon neutrinos traveling through the earth, the NOvA Experiment looks for the appearance of electron neutrinos, a transformation explained by the quantum-mechanical phenomenon known as neutrino oscillation. NOvA uses two neutrino detectors located 14.6 mrad off-axis from the main beam direction. The first (Near) detector stands at a distance of 1 km from the neutrino source, while the second (Far) one is at 810 km. Traveling from the Near Detector to the Far Detector, muon neutrinos can morph into electron neutrinos with a probability depending upon the parameters Δm^2_{32} and $\sin^2\theta_{23}$, among others. By comparing the observed number of ν_μ and ν_e events at the Far Detector with the expected number of events predicted by a 3-neutrino oscillation model, NOvA is able to measure these parameters and help to improve our understanding about neutrinos. After a brief introduction to the physics of neutrinos and a presentation of the experiment, in this talk the most recent results obtained by NOvA through the study of muon neutrino oscillations $\nu_\mu \to \nu_\mu$ and $\nu_\mu \to \nu_e$, are shown. The oscillation parameters are found to be $\Delta m^2_{32} = 2.44 \times 10^-3$ eV^2 and $\sin^2\theta_{23} = 0.56$.

1. Introduction

Neutrinos are elementary particles characterized by having no electric charge and 1/2-spin. As part of the Standard Model (SM) of particle physics, they are the neutral companions of the charged leptons, so making a group of three neutrinos (flavor states): ν_e, ν_μ, ν_τ. They interact only through the weak interaction, mediated by the $W^\pm$ and Z bosons, and are assumed to be massless in the SM (see, for instance, [1]).

Experimentally it has been stablished that neutrinos are able to change its flavor, a phenomenon known as neutrino oscillation, implying that, contrary to what the SM states, neutrinos are massive particles and states with definite flavor $(\nu_e, \nu_\mu, \nu_\tau)$ are a mixture of neutrinos with definite mass (ν_1, ν_2, ν_3). Models of neutrino masses and mixing, and its implications on physics beyond the SM have been studied widely studied [2–6], looking for an understanding of neutrino physics and its phenomenology.

Neutrino mixing is usually parametrized as

$$\begin{pmatrix} \nu_e \\ \nu_\mu \\ \nu_\tau \end{pmatrix} = R(\theta_{23}) \cdot R(\theta_{13}, \delta_{CP}) \cdot R(\theta_{12}) \begin{pmatrix} \nu_1 \\ \nu_2 \\ \nu_3 \end{pmatrix}; \quad (1)$$

$R(\theta_{ij})$ in Equation (1) are the orthogonal rotation 3×3 matrices presented in Equation (2):

$$R(\theta_{12}) = \begin{pmatrix} c_{12} & s_{12} & 0 \\ -s_{12} & c_{12} & 0 \\ 0 & 0 & 1 \end{pmatrix}, \quad R(\theta_{23}) = \begin{pmatrix} 1 & 0 & 0 \\ 0 & c_{23} & s_{23} \\ 0 & -s_{23} & c_{23} \end{pmatrix}, \quad R(\theta_{13}) = \begin{pmatrix} c_{13} & 0 & s_{13}e^{-i\delta_{CP}} \\ 0 & 0 & 1 \\ -s_{13}e^{i\delta_{CP}} & c_{13} & 0 \end{pmatrix}, \quad (2)$$

where $s_{ij} \equiv \sin\theta_{ij}$, $c_{ij} \equiv \cos\theta_{ij}$, and δ_{CP} is a phase which parametrizes the CP violation in the lepton sector.

This parametrization, and using the basics of quantum mechanics to compute the transition between neutrinos of different flavor, allows to find the probability that a neutrino created at the source with a flavor α is observed at the detector as a neutrino with flavor β after traveling a given distance L:

$$P_{\nu_\alpha \to \nu_\beta} = |\langle \nu_\beta | \nu_\alpha(L) \rangle| = \left| \sum_k U^*_{\beta k} \exp\left(-i \frac{m_k^2 L}{2E}\right) U_{\alpha k} \right|^2 \quad (3)$$

From the probability in Equation (3), it is clear that if neutrinos are massive, the oscillation probability is not null. Equation (3) also shows that the flavor transition depends on $\Delta m^2_{ij} \equiv m^2_i - m^2_j$ and not on the neutrino mass itself, indicating that this phenomenon would not give information about the absolute neutrino masses.

The mixing angles and the squared-mass differences have been precisely measured by experiments using neutrinos from the sun (θ_{12}, Δm^2_{12}), reactors (θ_{13}) and the atmosphere and accelerators (θ_{23}, Δm^2_{32}) (global neutrino-oscillation data analyses combining all available data can be found in [7, 8]).

2. The NOvA experiment

The NOvA (NuMI Off-axis ν_e Appearance) Collaboration brings together a group of around 250 scientist (professors, researchers, students) and engineers from 49 institutions across 7 countries. The NOvA experiment [9–11] is a two-detector long-baseline neutrino oscillation experiment looking for the appearance of (anti-)electron neutrinos from a beam of (anti-)muon neutrinos. Its main scientific goals include the search for answering the questions about the neutrino mass ordering, the measurement of CP-violating phase and the measurement of θ_{23}, by studying neutrino oscillations using the four channels depicted in Equation (4):

$$\begin{aligned} &\nu_\mu \to \nu_\mu, \qquad &&\nu_\mu \to \nu_e \\ &\bar{\nu}_\mu \to \bar{\nu}_\mu, \qquad &&\bar{\nu}_\mu \to \bar{\nu}_e \end{aligned} \quad (4)$$

The neutrino beam, which can be operated in either a neutrino or antineutrino mode, is created following the decay of charged pions to (anti-)muons and (anti-)neutrinos. In the neutrino mode, the whole chain results in a beam composed mainly by ν_μs (95%), with a small contamination of ν_es (1%) and $\bar{\nu}_\mu$s (4%). The energy spectrum of the beam as expected at the FD, separated by its composition is shown in Figure 1.

The NOvA neutrino detectors are functionally identical calorimeters consisting of cells filled with a liquid scintillator, organized in planes alternating in vertical and horizontal orientations. Events taking place in the cells may produce light which is collected by an optical fiber connected to an avalanche photodiode. The alternation of horizontal and vertical planes allows NOvA to have top and side views for each event as particle crossing different cells are detected by the energy deposited in them. In this way, it is possible to reconstruct the particle trajectory by following the created track up to the point where the event was originated (interaction point).

Thanks to the granularity of the detectors, the tracks left by the interacting particles (coming from the beam and cosmic rays) have been used by NOvA to implement an event selection and classification process based on image recognition techniques known as Convolutional Visual Network (CVN) [12]. This method is based on training a series of linear operations using simulated events, in order to extract their features to identify the topology of specific interaction, with special focus on neutrino-like events.

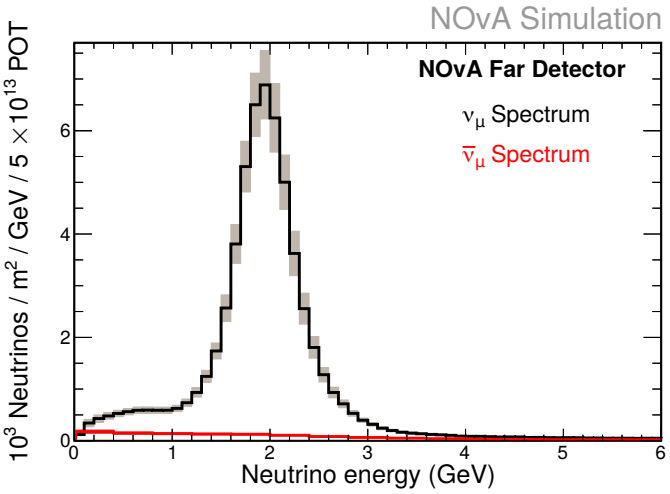

Figure 1. Number of neutrino events from the beam expected in the FD as a function of the neutrino energy.

The Far Detector (FD) is made by 896 planes, with a total mass of 14 kt. It is placed near Ash River, Minnesota, at 810 km from the neutrino source, at Fermilab, and at an angle of 14.6 mrad from the central axis of the neutrino beam, resulting in a neutrino flux with a narrow band energy distribution and peaked around 1.9 GeV (see Figure 2).

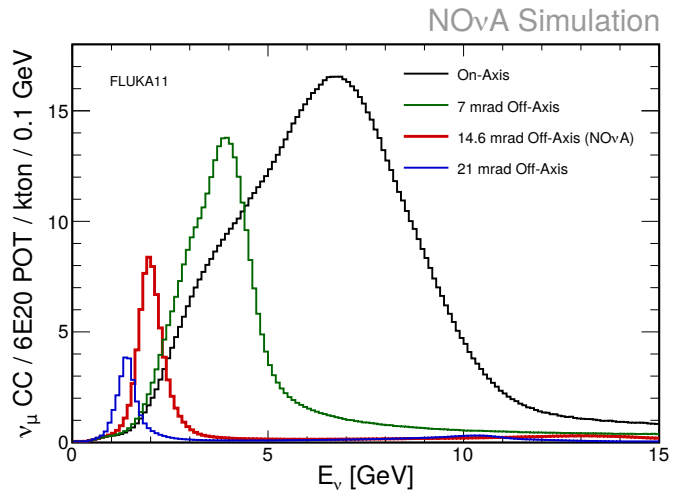

Figure 2. Neutrinos events energy distribution for different angles of the detector location with respect to the mean neutrino beamline.

The Near Detector (ND), on the other hand, consists of 214 planes with a mass of 290 *ton*, and is located at Femilab, 100 *m* underground (to reduce background from cosmic cays) and 1 km away from the neutrino source. Its position is such that the angle with respect to the main beam axis is the same as the FD, in order to obtain a similar neutrino energy spectrum to the one expected at the FD in the absence of oscillations.

IOP Conf. Series: Journal of Physics: Conf. Series **1219** (2019) 012021 doi:10.1088/1742-6596/1219/1/012021

3. Data analysis and results

3.1. Disappearance and appearance data

The results presented here were obtained by NOvA using data collected from February 2014 to February 2017, for a total of 8.85×10^{20} protons on target [11]. As mentioned above, NOvA has the possibility to study the disappearance of ν_μ or $\bar{\nu}_\mu$ and the appearance of ν_e or $\bar{\nu}_e$. Here, the results of the neutrino mode study are presented, and the measured values of the oscillation parameters from a joint (appearance-disappearance) analysis are reported.

Following a rigorous selection process (detailed description can be found in [11]), a total of 126 ν_μ events were observed in the FD with an energy distribution as shown in Figure 3. The figure compares the data (black dots with error bars) against the expected number of events under the hypothesis of neutrino oscillation (purple solid line). In the absence of oscillations, we would have expected to observe ~ 720 muon neutrino events, a clear indication of ν_μ disappearance.

The analysis performed by NOvA found that the most relevant region on the energy spectrum is around 1.6 GeV, where a sharp dip is observed. This is why the bin width is smaller in this part of the spectrum. A good (energy) location of the dip and its depth allows NOvA to get precise measurement of Δm^2_{32} and $\sin^2\theta_{23}$, respectively.

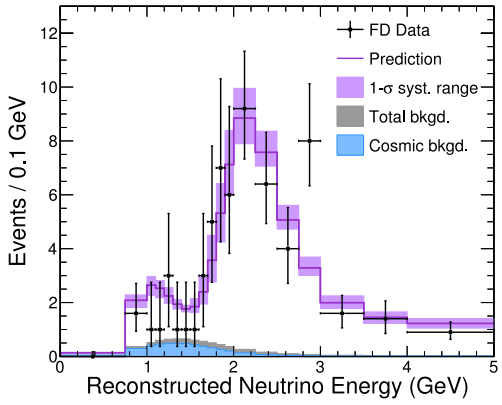

Figure 3. Comparison between the selected ν_μ event candidates in the FD data (dots) and the best fit prediction (solid-purple line). The purple band corresponds to the 1σ systematics uncertainty range [11].

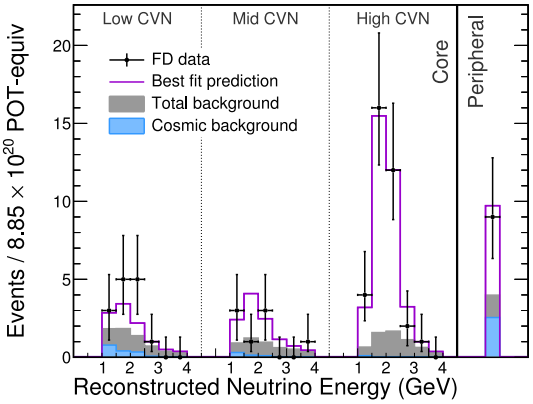

Figure 4. Comparison between the selected ν_e event candidates in the FD data (dots) and the best fit prediction (solid-purple line). The shaded spectra show the expected background [11].

Regarding the appearance of electron neutrinos, a total of 66 ν_e events were observed, while only 7 were expected from the beam. In this case, a specific and distinctive classification of data was used in order to extract the most information from them, after applying the selection processes, including CVN, which tags events from a value ranging from 0 (less ν_e-like event) to 1 (more ν_e-like event). The resulting energy distribution of the data is shown in Figure 4. Again, data (black dots) are compared against the best fit of the neutrino oscillation model (purple solid line), and the expected background is also shown. Like for the case of ν_μ disappearance, the prediction of neutrino oscillations is well in agreement with data, which is a clear indication of ν_es appearance from a beam mainly composed by ν_μs.

3.2. Joint data fit

A simultaneous fit to the data from ν_μ disappearance and ν_e appearance was performed by NOvA, including information about uncertainties from different sources (see details in [11]), in a suitable χ^2 function to be minimized with respect to the oscillation parameters. For the analysis, the effect that matter has on the oscillation is also considered by using the CRUST2.0 model [13] of the Earth density with $\rho = 2.84\text{g/cm}^3$, taking into account the depth of the NuMI beam (810 km) for the NOvA baseline.

The best fit of the oscillation parameters is found to be

$$\Delta m^2_{32} = 2.44 \times 10^{-3}\,\text{eV}^2, \qquad \sin^2\theta_{23} = 0.56, \qquad \delta_{\text{CP}} = 1.21\pi \tag{5}$$

The values in Equation (5) correspond to a normal mass ordering and the upper θ_{23} octant (i.e. $\theta_{23} > 45°$), with $\chi^2 = 86.4/72$ DOF (Degrees of Freedom). The minimization of the χ^2 function produce another local minimum close to the best fit (global minimum) also for normal mass ordering, but in the lower θ_{23} octant, with a difference of its χ^2 and the overall best fit $\Delta\chi^2 = 0.13$. On the other hand, the inverted mass hierarchy case results being largely disfavored.

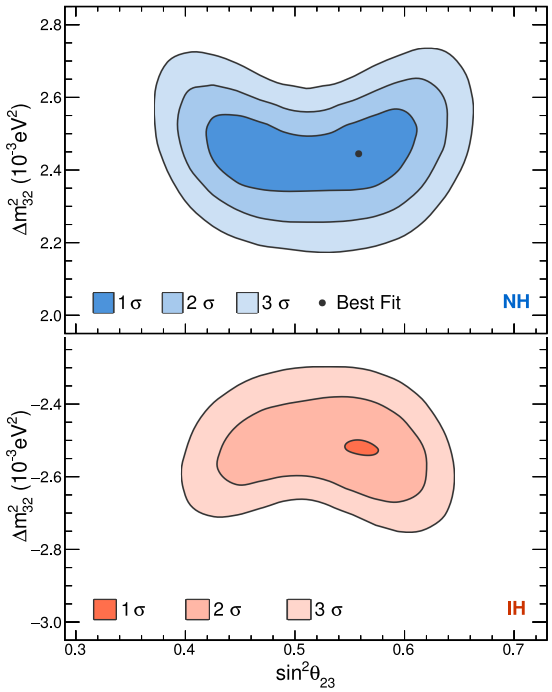

Figure 5. Allowed regions of the $(\Delta m^2_{32}, \sin^2\theta_{23})$ parameter space obtained from the joint analysis of ν_e appearance and ν_μ disappearance data. Different color intensity corresponds to different levels of significance. *Top*: normal mass ordering; *bottom*: inverted oredering [11].

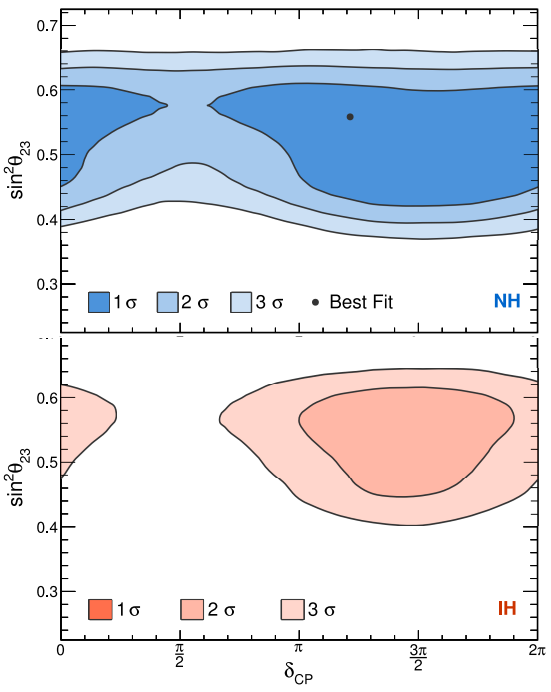

Figure 6. Allowed regions of the $(\sin^2\theta_{23}, \delta_{CP})$ parameter space obtained from the joint analysis of ν_e appearance and ν_μ disappearance data. Different color intensity corresponds to different levels of significance. *Top*: normal mass ordering; *bottom*: inverted oredering [11].

Figure 5 and Figure 6 show the 2-dimensional contours at 1, 2 and 3σ C.L. for the oscillation parameter spaces $(\Delta m^2_{32}, \sin^2\theta_{23})$ and $(\sin^2\theta_{23}, \delta_{CP})$, respectively. Upper plots correspond

to the normal mass ordering while bottom plots refer to inverted ordering. From them, 1-dimensional (1σ C.L.) allowed regions can be extracted for each parameter and the intervals are exhibited in Table 1 (for the normal mass ordering).

Table 1. $1\,\sigma$ confidence intervals for the oscillation parameters in the normal mass ordering [11].

Parameter (units)	$1\,\sigma$ interval(s)
Δm^2_{32} (10^{-3}eV^2)	[2.37, 2.52]
$\sin^2\theta_{23}$	[0.43, 0.51] and [0.52, 0.60]
δ_{CP} (π)	[0, 0.12] and [0.91, 2]

Among other features, the contour plots show that the normal mass ordering is preferred over the inverted one; this is evident by the fact that the red contours (bottom plots) are smaller than the blue ones, and that the 1σ region is very small (Figure 5) or even absent (Figure 6). It is noticeable that a large region around $\delta_{CP} = \pi/2$ for the inverted ordering, Figure 6 bottom plot, is excluded at $> 3\sigma$ C.L. Notice also that $\theta_{23} = 45°$ is excluded at a 0.8σ significance, which is different to what was reported previously by NOvA (2.6σ) [14]; this is given by the improvement of the event simulations and calibration, and also by the increased statistics.

Finally, Figure 7 shows a comparison of the results obtained by NOvA against other long-baseline experiments. The comparison is for the 90% C.L. allowed regions in the $(\Delta m^2_{32}, \sin^2\theta_{23})$ parameter space for the normal mass ordering case. The plot nicely shows that all the experiments are consistent between each other and all of them are concordant with $\theta_{23} = 45°$ i.e., maximal mixing.

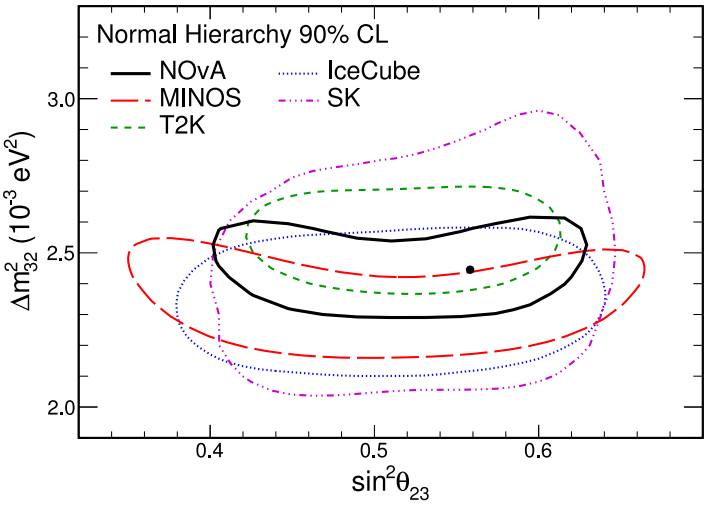

Figure 7. Comparison of the allowed regions of the Δm^2_{32} vs. $\sin^2\theta_{23}$ parameter space at the 90% C.L. obtained by different experiments: NOvA (black line; best-fit value, black point) [11], T2K [15] (green dashed), MINOS [16] (red dashed), IceCube [17] (blue dotted), and Super-Kamiokande [18] (purple dash-dotted).

As mentioned in Section 2, the neutrino beam can be operated in an anti-neutrino mode, too. NOvA has already performed an analysis of anti-neutrino data, and the first results were presented at the XXVIII International Conference on Neutrino Physics and Astrophysics (Neutrino 2018, https://www.mpi-hd.mpg.de/nu2018/) [19], and will be published in an upcoming paper.

4. Conclusions

NOvA has clearly observed the disappearance of muon neutrinos and the appearance of electron neutrinos from a beam primarily made of ν_μs. These observations are in good agreement with a three-neutrino oscillation model with the relevant parameters given in Equation (5), and allowed intervals as in Table 1. Data favor a normal mass ordering and an important region around $\delta_{CP} = \pi/2$ for the inverted ordering is excluded with a significance larger than 3σ; as a matter of fact, the inverted ordering is disfavored at the 95% C.L. overall. Finally, the NOvA results are consistent with maximal mixing in the $\mu - \tau$ sector, which is in concordance with other long-baseline neutrino oscillation experiments.

Acknowledgments

M.A.A. thanks the support given by Universidad del Atlántico through the Vicerrectoría de Investigaciones, Extensión y Proyección Social. The author also thanks to the Neutrino Physics Center (Fermilab) for the support provided through the "Neutrino Physics Center Fellowship" in the Spring 2016.

References

[1] Martínez R 2006 Las interacciones no gravitacionales *Momento* **32** 28
[2] Moreno A, Quimbay C 2004 Mezcla de neutrinos y mecanismo See-Saw *Momento* **28** 15
[3] Arrieta E, Nowakowski M 2006 Models of neutrino masses *Revista Colombiana de Física* **38** 1210
[4] Cataño E, Martínez R 2009 Bariogénesis a través de Leptogénesis *Momento* **39** 30
[5] Duarte J, Rodríguez J-Alexis and Martínez R 2009 Neutrinos en modelos 331 supersimétricos *Revista Colombiana de Física* **41** 213
[6] King S 2015 Models of neutrino mass, mixing and CP violation *J. Phys. G* **42** 123001 (*Preprint* arXiv:1510.02091 [hep-ph])
[7] de Salas P F, Forero D V, Ternes C A, Tortola M and Valle J W F 2018 Status of neutrino oscillations 2018: 3σ hint for normal mass ordering and improved CP sensitivity *Phys. Lett. B* **782** 633 (*Preprint* arXiv:1708.01186 [hep-ph])
[8] Esteban I, Gonzalez-Garcia M C, Maltoni M, Martinez-Soler I and Schwetz T 2017 Updated fit to three neutrino mixing: Exploring the accelerator-reactor complementarity *J. High Energy Phys.* **2017(87)** doi:10.1007/JHEP01(2017)087 (*Preprint* arXiv:1611.01514 [hep-ph])
[9] Ayres D S, *et al.* 2007 *The NOvA technical design report* (United States: Fermi National Accelerator Lab.) doi:10.2172/935497
[10] Adamson P *et al.* 2017 Constraints on oscillation parameters from ν_e appearance and ν_μ disappearance in NOvA *Phys. Rev. Lett.* **118** 231801 (*Preprint* arXiv:1703.03328 [hep-ex])
[11] Acero M A *et al.* 2018 New constraints on oscillation parameters from ν_e appearance and ν_μ disappearance in the NOvA experiment *Phys. Rev. D* **98** 032012 (*Preprint* arXiv:1806.00096 [hep-ex])
[12] Aurisano A *et al.* 2016 A convolutional neural network neutrino event classifier *Journal of Instrumentation* **11(09)** P09001
[13] Bassin C, Laske G, and Masters G 2000 The current limits of resolution for surface wave tomography in North America *Eos Trans. AGU* **81(48)** F897
[14] Adamson P *et al.* 2017 Measurement of the neutrino mixing angle θ_{23} in NOvA *Phys. Rev. Lett.* **118** 151802 (*Preprint* arXiv:1701.05891 [hep-ex])
[15] Abe K *et al.* 2017 Measurement of neutrino and antineutrino oscillations by the T2K experiment including a new additional sample of ν_e interactions at the far detector *Phys. Rev. D* **96** 092006 2018 Erratum: *Phys. Rev. D* **98** 019902 (*Preprint* arXiv:1707.01048 [hep-ex])
[16] Adamson P *et al.* 2014 Combined analysis of ν_μ disappearance and $\nu_\mu \to \nu_e$ appearance in MINOS using accelerator and atmospheric neutrinos *Phys. Rev. Lett.* **112** 191801 (*Preprint* arXiv:1403.0867 [hep-ex])
[17] Aartsen M G *et al.* 2018 Measurement of atmospheric neutrino oscillations at 656 GeV with IceCube DeepCore *Phys. Rev. Lett.* **120** 071801 (*Preprint* arXiv:1707.07081 [hep-ex])
[18] Abe K *et al.* 2018 Atmospheric neutrino oscillation analysis with external constraints in Super-Kamiokande I-IV *Phys. Rev. D* **97** 072001 (*Preprint* arXiv:1710.09126 [hep-ex])
[19] Sanchez M 2018 *NOvA results and prospects XXVIII International Conference on Neutrino Physics and Astrophysics (Heidelberg)* (Switzerland: Zenodo) doi: 10.5281/zenodo.1286758 url: https://doi.org/10.5281/zenodo.1286758